ACS Sustainable Chemistry & Engineering

pubs.acs.org/journal/ascecg

Research Article

Environmentally Friendly Sunscreens: Mechanochemical Synthesis and Characterization of β-CD Inclusion Complexes of Avobenzone and Octinoxate with Improved Photostability

Simone d'Agostino, Alessandra Azzali, Lucia Casali, Paola Taddei,* and Fabrizia Grepioni*

Cite This: *ACS Sustainable Chem. Eng.* 2020, 8, 13215−13225

Read Online

ACCESS | Metrics & More | Article Recommendations | Supporting Information

ABSTRACT: We report on the mechanochemical synthesis of inclusion complexes obtained by reacting β-cyclodextrin (β-CD) with two widely used sunscreens, namely, avobenzone (AVO) and octinoxate (OCT). Formation of crystalline inclusion complexes was confirmed via a combination of solid-state techniques, including X-ray diffraction (XRD), Raman, and ATR-FTIR spectroscopies. A new, metastable polymorph of avobenzone was also isolated and characterized. NMR spectroscopy and thermal analyses (TGA and DSC) allowed us to evaluate the host/guest ratio and the water content (ca. $8H_2O$) in crystalline $(\beta\text{-CD})_2\cdot$AVO and $(\beta\text{-CD})_3\cdot OCT_2$. Photodegradation of the two sunscreens upon inclusion in the hydrophobic cavity of β-CD was evaluated in solution via mass spectrometry (ESI-MS) and UV−vis spectroscopy and found to be sharply reduced. All findings indicate that the inclusion of AVO and OCT in β-CD might represent a viable route for the preparation of environmentally friendly sunscreens with improved photostability to be used in formulations of sun creams.

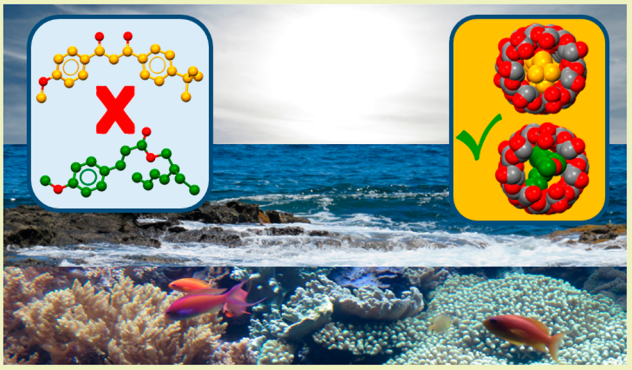

KEYWORDS: *Avobenzone, Octynoxate, Sunscreens, Cyclodextrins, Inclusion complexes, Mechanochemistry*

INTRODUCTION

Sun protection is widely used and valued for its importance in skin protection, as it can help in preventing skin cancer and photoaging, along with all the inflammatory effects that solar radiation can cause. It is well known that when UV radiation penetrates the stratum corneum, it can give rise to short-termed symptoms as well as long-term diseases.[1,2] It accelerates skin aging, promoting the formation of reactive oxygen species[3] and can cause DNA damage, erythema, inflammatory effects, pigment darkening, immunosuppression, reduced vitamin D production, and carcinogenesis.[4,5] It is thus of fundamental importance to efficiently protect the skin during sun exposure.

Ideally, a good sunscreen should be protecting from UVA and UVB light, should be photostable, and should not penetrate under the skin in order to avoid secondary effects. Furthermore, when a fraction of the active agents present in a sun cream is absorbed by the stratum corneum, its efficacy and protector factor are lowered, as the same concentration of UV filter is not maintained during the time of usage. Moreover, it should be easy to apply, anti-irritating, transparent to visible light (i.e., invisible on the skin), and subject to approval by the local regulatory agency.[4] Finally, it should not be harmful for the environment and wildlife when it is dispersed in natural waters.

Since none of the available sun creams satisfy all these requirements, many preparative efforts are being made toward formulations that better mimic an ideal sunscreen composition, in terms of components of the final product and of UV filters used as active agents.[6,7]

One of the biggest issues with organic UV filters is photostability, as it has been proved that under UV radiation some filters undergo cis−trans photoisomerization, keto−enol tautomerization or fragmentation reactions,[8] thus losing efficacy;[3,4,8−10] in addition to this, they can also promote undesirable reactions or chemically interact with the skin.[11−13]

The avobenzone and octinoxate filters (Scheme 1), which absorb mainly in the UVA and UVB regions, respectively, are among the most widely used and efficient filters added to sun creams, but they easily photodegrade and interact with one another via photocyclization,[9,11,14−19] forming byproducts that either absorb in a different UV range or present a lower molar

Received: April 10, 2020
Revised: July 8, 2020
Published: August 10, 2020

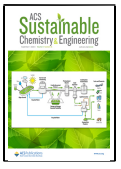

Downloaded via UNIV BOLOGNA on September 8, 2020 at 13:16:27 (UTC).
See https://pubs.acs.org/sharingguidelines for options on how to legitimately share published articles.

ACS Publications

© 2020 American Chemical Society

Scheme 1. Schematic Representation of Reagents Used in This Work: UVA Filter Avobenzone (AVO), UVB Filter Octinoxate (OCT), and β-Cyclodextrin (β-CD)

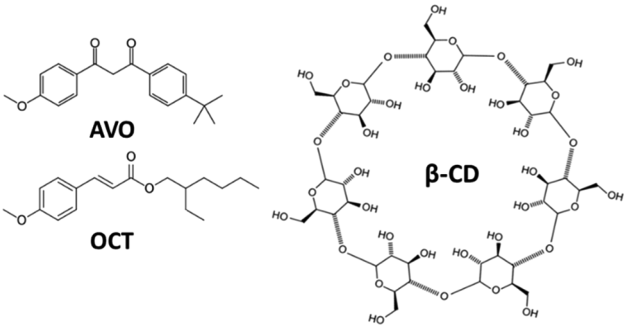

absorption coefficient. In particular, octinoxate undergoes photoisomerization from E-octinoxate to Z-octinoxate, where the former isomer is the desired component in sunscreens, as it is characterized by a higher molar absorption coefficient in a number of solvents.[14] For avobenzone, instead, photostability is highly dependent on the polarity and proticity of the solvent;[16,20,21] it is usually found as a physical mixture of the keto and the enol forms but, upon irradiation, transforms into the pure diketo form, which absorbs in the UVC range.[8] Moreover, avobenzone degrades to radical fragments.[8,20,22]

New formulations need to be proposed with high and constant photoprotection efficiency for the lifespan of the sun cream. It is of common use in the pharmaceutical field to adjust the photostability of a formulation by means of additives, e.g., esters or polymer matrices,[23−26] or additional UV filters.[27] The new components, however, might impact on the photoreactivity of the original filter or on the environment.[9,28] In recent years, a number of sunscreens have been proved to be harmful for corals and sea life,[29−31] as sun creams applied on human skin can be washed off in natural water or in the shower or it can be absorbed by the skin and excreted with urine.[27,32] This recently led some islands (Palau,[33] Hawaii,[34] and Virgin Islands, among others) to take action and ban a series of UV filters starting in 2020.[35−37] UV filters are considered to contribute to coral bleaching, depression of the coral reproductive system, and damage and deformation of coral larvae,[29] and their action is worsened in warm waters. They can also be found in marine biota including fish and molluscs, affecting their endocrine system and inducing reproductive pathologies.[38,39] It is estimated that between 6000 and 14,000 tons of sunscreens are washed into the oceans every year, with 10% of global coral reefs being at risk of exposure.[40] Also, sun creams are not the only relevant cause of contamination, as UV filters are added also to lip balms, moisturizers, shampoos, and other cosmetic products.[3,41]

Encapsulation or addition of antioxidants are among the solutions proposed by researchers for the stabilization of photosensitive drugs.[7,42] Research on encapsulation is mainly focused on cyclodextrins, which are known to form a great number and variety of inclusion compounds, being at the same time not expensive and unharmful to the environment.

Cyclodextrins are cyclic oligosaccharides with a variable number of glucose units, generally 6 (α-cyclodextrins), 7 (β-cyclodextrins), or 8 (γ-cyclodextrins), bonded via α-1,4 glycosidic bonds. They possess a hydrophilic surface that makes them soluble in water, and a hydrophobic cavity, which can be filled by relatively small and apolar organic molecules. As a result of these properties, cyclodextrins have been widely employed as drug carriers in the pharmaceutical field and have been investigated for applications in the food industry and in the environmental[43,44] and cosmetics sciences.

Encapsulation of sunscreens in cyclodextrins has been investigated in the last decades,[45−47] and stable inclusion complexes have been obtained with useful applications in many fields, ranging from cosmetics[20,21,48] to inks technology[49] and fabrics,[50] with enhanced properties of the included filters with respect to photostability, water solubility, and skin penetration; they can prevent the permeation of UV filters in the stratum corneum and keep a more constant protection factor at the skin surface.[1,12,51,52]

In the present work, we report on the preparation by mechanochemical methods[53] of β-cyclodextrin (β-CD) inclusion complexes with the sunscreens avobenzone (AVO) and octinoxate (OCT) (Scheme 2).

Scheme 2. Syntheses (Water as Liquid Medium) and Characterization Techniques Employed for the Inclusion Compounds Discussed in This Work

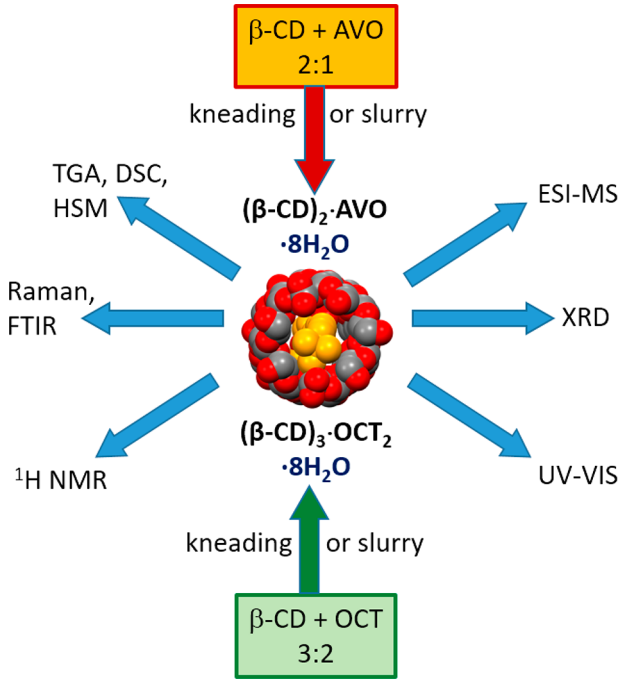

The products are both hydrates with an approximate content of eight water molecules; for sake of conciseness, however, throughout this work, they will be indicated with the formulas (β-CD)$_2$·AVO and (β-CD)$_3$·OCT$_2$. The two compounds were fully characterized by a combination of techniques, including X-ray diffraction (XRD), thermogravimetric analysis (TGA), NMR, and FTIR and Raman spectroscopies; the photostability of avobenzone and octinoxate encapsulated within the β-cyclodextrins was evaluated via mass spectrometry (MS) and UV−vis spectrophotometry and found to be strongly enhanced with respect to the unprotected molecules. A new, metastable polymorph of avobenzone, Form II, was also isolated and characterized, which is monotropically related to the commercially available Form I.

This study would have an immediate impact on the formulation of sun creams by (i) improving the photostability of the two efficient UV filters via inclusion in a harmless

https://dx.doi.org/10.1021/acssuschemeng.0c02735
ACS Sustainable Chem. Eng. 2020, 8, 13215−13225

excipient as β-cyclodextrin, (ii) possibly reducing the stratum corneum permeation, and (iii) maintaining constant the concentration of the UV filters at skin level, thus reducing the amount of sun cream to be used, with a positive impact on the environment. The mechanochemical preparation of these inclusion compounds also complies with the principles of green chemistry.

EXPERIMENTAL SECTION

Materials. All reagents were purchased from Sigma-Aldrich and used without further purification. Double distilled water and reagent grade solvents were used. All solid materials were preliminarily screened for chemical and crystal phase purity via XRPD analysis. In the diffraction pattern of the commercial form of avobenzone, an extra peak was detected at a low angle (see Figure SI-5) that could not be attributed to the known Form I (CSD refcode WEBGAL). This prompted us to perform a polymorph screening for avobenzone, which allowed us to identify, isolate, and characterize the new, metastable Form II (Supporting Information).

Synthesis. *Mechanochemical Synthesis.* The inclusion complex $(\beta\text{-CD})_2\cdot$AVO was obtained by ball milling $\beta\text{-CD}\cdot 10H_2O$ (89.44 mg, 0.068 mmol) and avobenzone (10.55 mg, 0.034 mmol) with the addition of a few drops of water for 60 min at 20 Hz in an agate jar. The same procedure was employed to prepare the inclusion complex $(\beta\text{-CD})_3\cdot OCT_2$, starting from 3:2 physical mixtures of $\beta\text{-CD}\cdot 10H_2O$ (87.16 mg, 0.066 mmol) and octinoxate (12.83 mg, 0.044 mmol).

Slurry. Powders of the inclusion complexes suitable for the Pawley refinement were obtained through slurry experiments. Water was added dropwise to a physical mixture of $\beta\text{-CD}\cdot 10H_2O$ and avobenzone (10.55 mg, 0.034 mmol) weighed in a 2:1 stoichiometry. When a suspension was obtained, the addition of water was interrupted; the suspension was then stirred for 10 days at ambient conditions, then filtered under vacuum. A pure inclusion complex was recovered as a white powder. The same procedure was employed to prepare the inclusion complex $(\beta\text{-CD})_3\cdot OCT_2$, starting from a 3:2 physical mixture of $\beta\text{-CD}\cdot 10H_2O$ and octinoxate.

Single Crystal Growth. Growth of crystals of both inclusion complexes was attempted by liquid−liquid diffusion of a solution containing β-CD in distilled water and a solution containing avobenzone or octinoxate in ethyl acetate. Single crystals suitable for XRD were obtained only for the avobenzone β-CD inclusion complex, $(\beta\text{-CD})_2\cdot$AVO.

X-ray Diffraction. *Single Crystal X-ray diffraction.* Single-crystal data for avobenzone Form II were collected at RT with an Oxford X'Calibur S CCD diffractometer equipped with a graphite monochromator (Mo Kα radiation, λ = 0.71073 Å). Data for the inclusion complex $(\beta\text{-CD})_2\cdot$AVO were collected at low temperature (100 K) on a Bruker D8 Venture diffractometer equipped with a PHOTON III detector, a IμS 3.0 microfocus X-ray source (Cu Kα radiation, λ = 1.54056 Å), and a cryostat Oxford CryoStream800. The structures were solved by intrinsic phasing with SHELXT[5] and refined on F^2 by full-matrix least-squares refinement with SHELXL implemented in the Olex2 software.[6] All nonhydrogen atoms were refined anisotropically. H_{CH} atoms for all compounds were added in calculated positions and refined riding on their respective carbon atoms. Data collection and refinement details are listed in Table S1. The guest avobenzone and the disordered water molecules in the structure of $(\beta\text{-CD})_2\cdot$AVO could not be unambiguously determined because of severe disorder; therefore, their contribution to the calculated structure factors was removed by using the Solvent Mask function implemented in the Olex2 software.[54] The program Mercury[55] was used to calculate the powder patterns from single crystal data and for molecular graphics. Crystal data can be obtained free of charge via www.ccdc.cam.ac.uk/conts/retrieving.html (or from the Cambridge Crystallographic Data Centre, 12 Union Road, Cambridge CB21EZ, UK; fax: (+44)1223−336−033; or e-mail: deposit@ccdc.cam.ac.uk). CCDC numbers 1990013−1990014.

Powder X-ray Diffraction. For phase identification purposes, XRPD patterns were collected on a PANalytical X'Pert Pro Automated diffractometer equipped with an X'celerator detector in Bragg−Brentano geometry, using Cu Kα radiation (λ = 1.5418 Å) without a monochromator in the 3°−40° 2θ range (step size, 0.033°; time/step, 20 s; soller-slit, 0.04 rad; antiscatter slit, 1/2; divergence slit, 1/4; 40 mA; 40 kV). The program Mercury[55] was used for simulation of XRPD patterns on the basis of single crystal data determined in this work or retrieved from the CSD.[56] Chemical and structural identities between bulk materials and single crystals were always verified by comparing experimental and simulated powder diffraction patterns (Supporting Information). For Pawley refinement purposes, XRPD patterns were collected on a PANalytical X'Pert PRO automated diffractometer with transmission geometry, equipped with a focusing mirror and pixcel detector, in the 2θ range 3°−70° (step size, 0.02608; time/step, 200 s; soller-slit, 0.02 rad; 40 kV; 40 mA). Powder diffraction data were analyzed with the software TOPAS4.1.[57] A shifted Chebyshev function with eight parameters was used to fit the background; see the Supporting Information for difference pattern plots and the associated Figures of Merit (FOM).

^{1}H NMR Spectroscopy. ^{1}H NMR spectra were recorded on a Varian INOVA 400 (400 MHz) spectrometer; the solvent used was dimethyl sulfoxide-*d*6 (DMSO-*d*6), bought from Sigma-Aldrich. All solutions were prepared with polycrystalline samples obtained via slurry. Chemical shifts are reported in ppm, with tetramethylsilane as the internal reference standard.

Raman Spectroscopy. Raman spectra were recorded on a Bruker MultiRam FT-Raman spectrometer equipped with a cooled Ge-diode detector. The excitation source was a Nd^{3+}-YAG laser (1064 nm) in the backscattering (180°) configuration. The focused laser beam diameter was about 100 μm, and the spectral resolution was 4 cm^{-1}. The spectra were recorded with a laser power at the sample of about 60 mW.

IR Spectroscopy. Attenuated total reflectance Fourier transform IR (ATR-FTIR) spectra were obtained using a Bruker Alpha FT-IR spectrometer. For the inclusion complexes, ATR-FTIR spectra were run on polycrystalline samples obtained via slurry, while for all the reactants measurements were run on the commercially available products.

Thermogravimetric Analysis (TGA). TGA measurements on all samples were performed with a PerkinElmer TGA7 thermogravimetric analyzer in the 30−400 °C temperature range under an N_2 gas flow and at a heating rate of 5.00 °C min^{-1}.

Differential Scanning Calorimetry (DSC). DSC traces were recorded using a PerkinElmer Diamond differential scanning calorimeter. All samples [10 mg of β-CD, avobenzone, octinoxate, $(\beta\text{-CD})_2\cdot$AVO and $(\beta\text{-CD})_3\cdot OCT_2$] were placed in open Al pans. All measurements were conducted in the 40−200 °C temperature range at a heating rate of 5.00 °C min^{-1}.

Hot Stage Microscopy. Hot stage experiments were carried out using a Linkam TMS94 device connected to a Linkam LTS350 platinum plate and equipped with polarizing filters. Images were collected with the imaging software Cell from an Olympus BX41 stereomicroscope.

UV−Vis Spectroscopy. UV−vis spectra were recorded with an Agilent Cary 60 UV−vis spectrophotometer. All solid samples were dissolved in a water/acetonitrile (50/50) solvent mixture at a concentration of 0.028 mM.

Mass Spectrometry. Mass spectra were recorded on a EVO G2-XS QTOF in positive mode. Solutions of inclusion complexes, avobenzone, and octinoxate were prepared in a 50:50 water:-acetonitrile solvent mixture HPLC grade, with a concentration of 5 mM for the inclusion complexes and 56 mM for avobenzone and octinoxate. The former was first dissolved in water. Then, acetonitrile was added in order to prevent the disassembling of the host/guest system, while the two UV filters were first dissolved in acetonitrile, and then, water was added.

RESULTS AND DISCUSSION

Inclusion Complexes: Synthesis and Solid-State Characterization. We have focused our attention on the

https://dx.doi.org/10.1021/acssuschemeng.0c02735
ACS Sustainable Chem. Eng. 2020, 8, 13215−13225

preparation of the inclusion complexes via mechanochemistry and slurry. To this end, β-cyclodextrin and avobenzone or octinoxate were ground together in 1:1 and 2:1 molar ratios with (kneading) and without (grinding) a catalytic amount of water. The grinding process was not successful, as it always resulted in a physical mixture of the reagents. The kneading process, on the contrary, yielded new solid forms: in the case of AVO, a mixture of a new phase and AVO was obtained for a 1:1 stoichiometric ratio, while a pure phase was obtained with a 2:1 stoichiometric ratio (Figure 1).

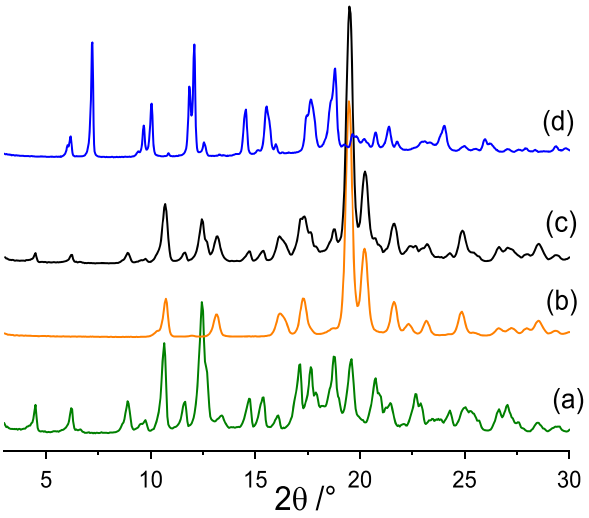

Figure 1. Comparison of the XRPD patterns for (a) β-CD, (b) AVO, (c) the product of the 2:1 grinding process, and (d) the product of the 2:1 kneading process (with water).

When β-CD and AVO were kneaded in a 1:1 stoichiometric ratio, the resulting polycrystalline powders contained, invariably, a mixture of a new phase, i.e., the inclusion complex, and AVO. On the other hand, pure phases were obtained only when the kneading was repeated in a 2:1 stoichiometric ratio. This strongly suggests the formula $(\beta\text{-CD})_2$·AVO for the inclusion complex; the degree of hydration was assessed via thermal analysis (see below).

Unfortunately, similar reasoning cannot be applied to octinoxate (see the Supporting Information for details of the reaction between OCT and β-CD), which is liquid and not detectable as an unreacted substance via X-ray diffraction. The stoichiometric ratio and water content, however, were successfully determined via spectroscopic methods and thermal analysis (see below).

Polycrystalline samples of fairly good quality for XRPD could be obtained via slurry (see the Experimental Section for details); similar unit cell parameters could be obtained for both inclusion compounds in the C2 space group (see the Experimental Section and Supporting Information for details), suggesting that, upon encapsulation of the sunscreens, the β-CD molecules adopt a common channel-type structure (see Figure 2 for the case of $(\beta\text{-CD})_2$·AVO) able to host avobenzone and octinoxate molecules. This is in agreement with what was reported in the work by Caira[58,59] on isostructural series: within each series, regardless of the guest, the packing arrangement of the β-CD molecules is the same, with almost identical unit cell parameters and fairly superimposable XRPD patterns. Our inclusion complexes fall in the C2 isostructural series. Similar conclusions can be drawn

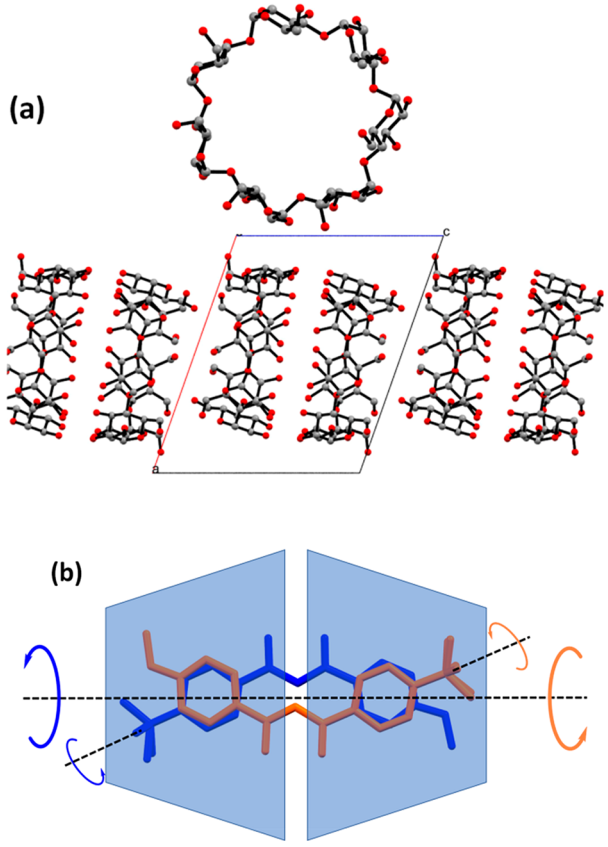

Figure 2. (a, top) Molecular structure of β-CD and (a, bottom) crystal packing of $(\beta\text{-CD})_2$·AVO showing the channel-like structure formed by the host molecule and extending along the *c*-axis. (b) Scheme of positional disorder for AVO (orange and blue molecules) within the β-CD hosts (light blue) likely to occur in $(\beta\text{-CD})_2$·AVO. H atoms and water molecules omitted for clarity.

for $(\beta\text{-CD})_3$·OCT_2. If β-CD was crystallized in the absence of AVO or OCT, however, only monoclinic $P2_1$ crystals, corresponding to the hydrated form of β-CD, were invariably obtained.

The β-CD:sunscreen ratio in the two inclusion complexes was assessed by solution ^{1}H NMR spectroscopy. On the basis of the relative integration of some diagnostic peaks for β-CD, AVO, and OCT (Supporting Information), the two inclusion complexes can be formulated as $(\beta\text{-CD})_2$·AVO and $(\beta\text{-CD})_3$·OCT_2. It is worth noting that a 2:1 stoichiometry was reported also for an inclusion complex of (2-hydroxy)propyl-β-cyclodextrin with avobenzone.[60] However, conclusive evidence of the water conten could not be obtained by this spectroscopy.

Thermal analyses, TGA and DSC, provided further evidence for the encapsulation products and were successfully employed to evaluate their water content. Avobenzone and octinoxate are stable up to 280 and 240 °C, respectively, while the TGA trace for hydrated β-CD shows a loss of weight, corresponding to dehydration, in the 40−80 °C range and complete degradation starting at ca. 300 °C. The two β-CD inclusion complexes are hydrated: a weight loss corresponding to ca. eight water molecules can be evaluated for both complexes, which are then stable up to ca. 300 °C. This indicates that inclusion of the UV filters into β-CD enhances their thermal stability, and their degradation is concomitant to that of β-CD (Supporting Information). Properties like melting, evaporation, or sublimation points of guest molecules are expected to vary

https://dx.doi.org/10.1021/acssuschemeng.0c02735
ACS Sustainable Chem. Eng. 2020, 8, 13215−13225

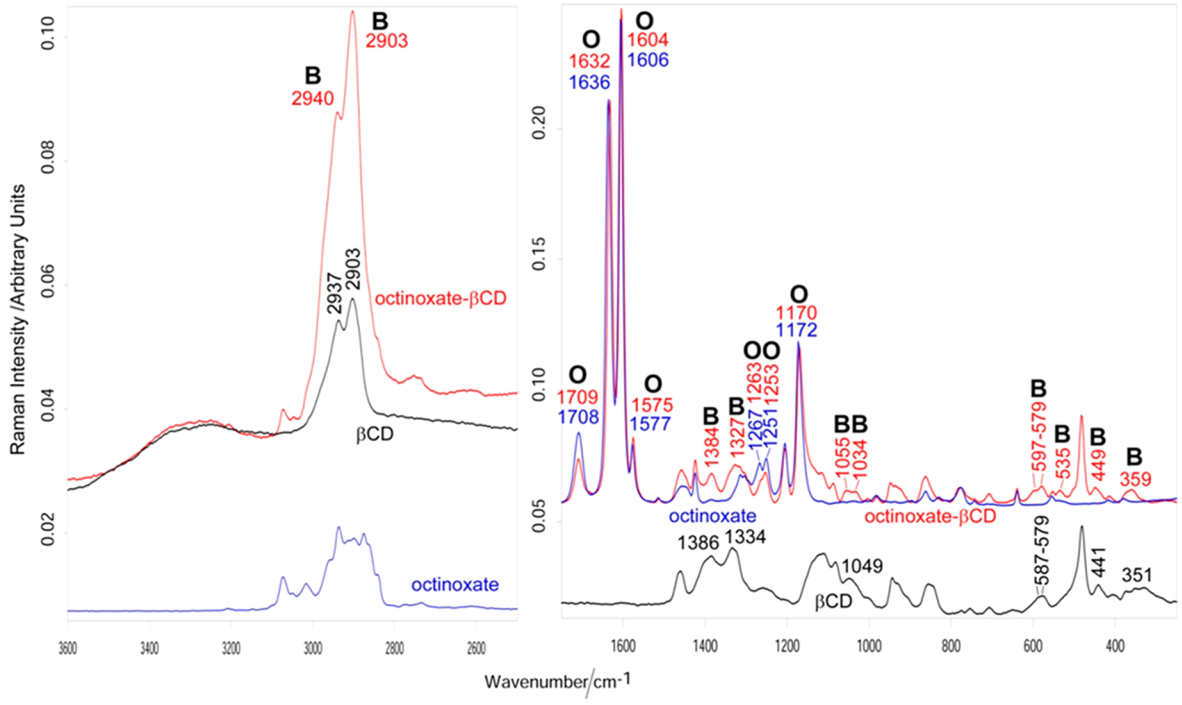

Figure 3. Raman spectra of the $(\beta\text{-CD})_3\cdot OCT_2$ inclusion complex, octinoxate, and β-CD. For sake of clarity, the main bands of octinoxate and β-CD that underwent changes upon formation of the inclusion compound are indicated with O and B, respectively.

substantially upon encapsulation by β-CD molecules.[61−65] In the case of $(\beta\text{-CD})_2\cdot$AVO, this behavior is particularly evident from the DSC trace, as no endothermic peak is observed up to decomposition, while pure avobenzone melts at 87 and 76 °C for Forms I and II, respectively (Supporting Information). On the other hand, for the octinoxate, which is liquid at ambient conditions, DSC measurements cannot be used to support the inclusion phenomenon. However, analogously to what was observed for $(\beta\text{-CD})_2\cdot$AVO, the DSC trace for the $(\beta\text{-CD})_3\cdot OCT_2$ inclusion complex (Supporting Information) shows a broad peak in the range of 50−90 °C, corresponding to the dehydration process.

To unambiguously confirm the host/guest ratios, we also attempted to grow single crystals for both $(\beta\text{-CD})_2\cdot$AVO and $(\beta\text{-CD})_3\cdot OCT_2$. Unfortunately, we succeeded only with the former, although crystals were tiny and poorly diffracting. Single crystal analysis confirmed the unit cell parameters and the monoclinic C2 space group previously determined via powder diffraction, but we were unable to fully model the structure, because of the static and dynamic disorders affecting the avobenzone molecule inside the hydrophobic cavity of β-CD, which, on the other hand, could be easily located and successfully refined. The cyclodextrin molecules in crystalline $(\beta\text{-CD})_2\cdot$AVO are packed in a channel-like structure (Figure 2), also observed in other complexes that crystallize in the same C2 isostructural series.[66−68] These disorder features inside the cavity of β-CD are supported by the following: (i) Both avobenzone Form I (CDS refcode WEBGAIL) and the new Form II experience disorder of the t-butyl moieties. (ii) Solution ^{1}H NMR measurements clearly show how pure avobenzone exhibits keto−enol tautomerization (Supporting Information). (iii) The volume of the β-CD cavity is large enough that rotation around the avobenzone main axis might also take place (see Figure 2 for a representation of the resulting disorder). Analogous behavior is expected for OCT in $(\beta\text{-CD})_3\cdot OCT_2$.

Raman and IR Spectroscopy. To additionally prove encapsulation of the sunscreens and to gain more insights about the potential keto−enol tautomerization of the avobenzone that might occur within $(\beta\text{-CD})_2\cdot$AVO, we also performed detailed Raman and IR studies. Figure 3 reports the Raman spectra of $(\beta\text{-CD})_3\cdot OCT_2$ as obtained via slurry, β-CD, and octinoxate.

As also detailed in Table SI-2, in the spectrum of the inclusion compound, the bands of both the components were observed, and several spectral features appeared shifted in wavenumber position and changed in relative intensity with respect to pure components. The main bands of octinoxate that underwent changes are indicated and are assigned[69] to C═O stretching (at about 1710 cm^{-1}), exocyclic C═C stretching (at about 1635 cm^{-1}), ring stretching (at about 1605 and 1575 cm^{-1}), ester and methoxy C−O stretching (at about 1265−1250 cm^{-1}, with change in band profile), and CH bending (at about 1170 cm^{-1}). The relative intensity of the bands at about 1635−1605 cm^{-1} changed a little; a similar behavior as well as a shift of the C═O stretching band have been reported upon dissolution of octinoxate in solvents of different polarities.[69] Therefore, the trend of the spectra indicates a change in the environment experienced by octinoxate upon formation of the inclusion compound. The variations in the ring stretching region suggest that also changes in van der Waals and hydrophobic interactions could have occurred. As also detailed in Table SI-2, several bands assignable to β-CD underwent shifts as well as changes in relative intensity and spectral profile; the main ones are indicated in Figure 3 and are assigned to CH stretching (at about 2940 and 2905 cm^{-1}, change in the band profile), CH bending (at about 1385 cm^{-1}), OH in plane bending (at about 1330 cm^{-1}), coupled CC and CO stretching (in the 1030−

https://dx.doi.org/10.1021/acssuschemeng.0c02735
ACS Sustainable Chem. Eng. 2020, 8, 13215−13225

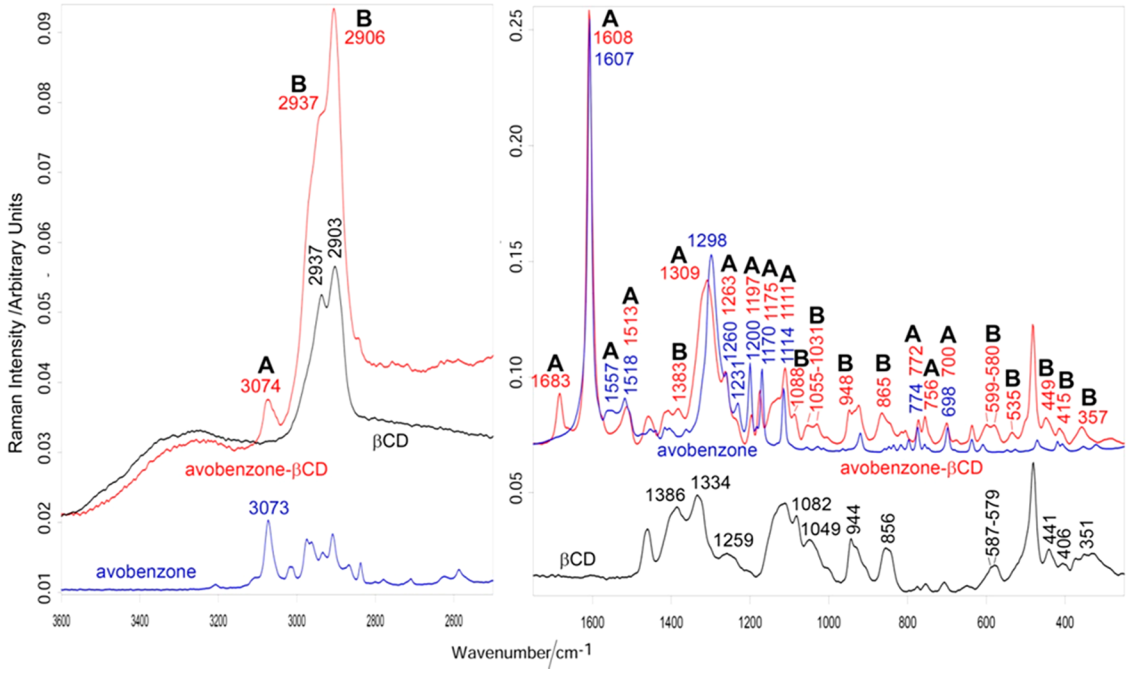

Figure 4. Raman spectrum of $(\beta\text{-CD})_2$·AVO, avobenzone and β-CD. For sake of clarity, the main bands of avobenzone and β-CD that underwent changes upon formation of the inclusion compound are indicated with A and B, respectively.

1050 cm^{-1} range), and ring and skeletal vibrations (in the 300−600 cm^{-1} range).[70] In the latter range, a band at 535 cm^{-1} appeared; it is probably ascribable to β-CD, in view of the fact that it appeared also in the spectrum of the inclusion compound with avobenzone (see below). The discussed trends showed the occurrence of interactions between octinoxate and β-CD, which is confirmed by the comparison between the spectra of the inclusion compound and the 3:2 physical mixture (Figure SI-14). The latter spectrum closely resembles the sum of the individual spectra of the guest and host molecules (Figure SI-15). The spectrum of the inclusion complex is different from that of the 3:2 physical mixture in the same ranges as described above in the text. Moreover, it is interesting to note that the bands assignable to the ring and skeletal vibrations of β-CD appeared strengthened. The IR spectrum of $(\beta\text{-CD})_3$·OCT_2 confirmed the above-reported Raman findings, as Figure SI-16 shows the bands of both octinoxate and β-CD components. Several bands of both host and guest molecules underwent wavenumber shifts upon formation of the inclusion compound, mainly in the same spectral ranges previously observed in Raman spectra.

Figure 4 reports the Raman spectra of $(\beta\text{-CD})_2$·AVO, β-CD, and avobenzone. As also detailed in Table SI-3, in the spectrum of the inclusion compound, the bands of both the components were observed. Upon formation of the inclusion compound, several bands assignable to both components changed in wavenumber position, relative intensity, and spectral profile.

The main bands assignable to avobenzone that underwent changes are indicated in Figure 4. New bands assignable to this component appeared (see, for example, the band at 1683 cm^{-1}), while others disappeared or noticeably decreased in intensity, due to the interaction with β-CD. In dibenzoylmethane, taken as the model compound, the band at about 1600 cm^{-1} has been assigned to C═O stretching[69,71] or ring stretching coupled to C−C−C═O asymmetric stretching[72] and may be attributed accordingly to pure avobenzone. This low wavenumber value, lower than those for benzoylacetone and acetylacetone, may be explained by considering that phenyl groups determine an enhancement of π-electron conjugation in the enol ring.[72] The appearance of the band at 1683 cm^{-1} in the spectrum of the inclusion compound suggests that a certain amount of the diketo tautomer formed inside the cavity of the β-CD. Actually, according to the literature on β-diketones,[73] a band in the 1800−1650 cm^{-1} range has been identified as a marker of the β-diketone form of curcumin;[74,75] the blue shift of this band with respect to the enol form may be explained by considering that the CO bond strengthens and thus shifts to higher wavenumbers upon loss of conjugation. As detailed in Table SI-3, upon formation of the inclusion complexes, other changes in the avobenzone bands concern several vibrational modes (Figure 4): aromatic CH stretching (at about 3070 cm^{-1}), ring stretching coupled to C−C−C═O and OH bending (1560−1500 cm^{-1} range),[69,72] C−O stretching (at about 1300 cm^{-1}),[69] methoxy C−O stretching (at about 1260−1230 cm^{-1}),[69] C−O−C methoxy bending (at about 1200 cm^{-1}),[69] CH bending and CO stretching (at about 1170 and 1110 cm^{-1}),[69,72] and CH out-of-plane bending and ring deformation (780−700 cm^{-1} range).[72] A certain broadening of several bands was observed upon formation of the inclusion compound. Also the bands of β-CD underwent some changes. The main ones occurred in the same spectral ranges above cited and are indicated in Figure 4; detailed assignments are reported in Table SI-3. This trend suggests that interactions occurred between avobenzone and β-CD, as also confirmed by the comparison between the spectra of the inclusion compound and the 2:1 physical mixture (Figure SI-17), with the latter resembling the sum of the individual spectra of the guest and host molecules (Figure SI-18). Also, in this case, the spectrum of the inclusion complex is different from that of the 2:1 physical mixture in the same ranges as described above. Moreover, it is interesting to

https://dx.doi.org/10.1021/acssuschemeng.0c02735
ACS Sustainable Chem. Eng. 2020, 8, 13215−13225

note, as observed for $(\beta\text{-CD})_3\cdot OCT_2$, that the bands assignable to the ring and skeletal vibrations of β-CD appeared strengthened.

The IR spectrum of $(\beta\text{-CD})_2\cdot$AVO (Figure SI-19) shows the bands of both avobenzone and β-CD components, although it is dominated by the bands of the host. The bands of the guest molecule were observed as weak spectral features. Detectable wavenumber shifts in several bands of both avobenzone and β-CD were observed upon formation of the inclusion complex, as previously observed in Raman spectra.

The vibrational results are in agreement with the literature. It is not surprising that changes in the guest ring modes were observed; actually, both octinoxate and avobenzone have been reported to penetrate into the hydrophobic cavity of β-CD[76] and γ-CD.[77] Molecular modeling studies for the inclusion complex have shown that the predominant contribution to the $E_{binding}$ comes from the van der Waals forces.[78] On the other hand, NMR studies in solution have shown that the aromatic portion of the octinoxate molecule is located inside the β-CD cavity, with the ester group close to the external surface of the macrocycle,[79] in agreement with Scalia et al.[47] Therefore, it is not surprising that upon inclusion compound formation only a slight shift of the C═O stretching mode was observed. Raman results showed also that avobenzone underwent tautomerization upon inclusion in β-CD, and a little amount of the diketone tautomer formed. Similar results have been reported by other authors upon inclusion of curcumin in γ-CD.[80,81] The keto form, being less polar than the enol form, may become stabilized in nonpolar solvents and in the slightly nonpolar interior of CDs,[82] which have been found to stabilize the least polar isomer.[80,81,83]

Photostability Studies of Inclusion Complexes. The effect of the inclusion complex formation on the photostability of the two sunscreens avobenzone and octinoxate was also investigated via a combination of ESI-MS mass spectrometry and UV−vis spectroscopy.

The mass spectrum of a mixture of $(\beta\text{-CD})_2\cdot$AVO and $(\beta\text{-CD})_3\cdot OCT_2$ (Figure SI-18, Table SI-4) previously synthesized was recorded. In order to prove photostability, the same sample was irradiated for 24 h under UV light, and then, it was analyzed again via mass spectrometry (Figure SI-19).

To prove the photostability of β-cyclodextrin complexes, peaks at around 600 m/z were analyzed, as the photodegradation is expected to form, via cycloaddition, the adduct of AVO and OCT weighing ca. 600 g/mol.[17]

Photostability was therefore verified via MS/MS tandem mass spectrometry for the sample containing irradiated $(\beta\text{-CD})_2\cdot$AVO and $(\beta\text{-CD})_3\cdot OCT_2$. In fact, when analyzing the spectra with lower collision energy, i.e.. 6 eV, a peak at 623 m/z appeared, while with a collision energy of 12 eV it decreased with a concomitant increase of the molecular peaks at 313 and 333 m/z, respectively, identifying OCT and AVO (Figure 5). This means that the presence of the peak at 623 m/z revealed the two noncovalently bonded UV filters together with a Na^+ ion at a lower collision energy. The photoprotection by β-cyclodextrins is thus efficient enough to avoid the dimerization of the sunscreens when the latter are included.

Analyses on the nonprotected UV filters were also conducted in order to verify the presence of the cycloadducts formed after irradiation. More details on the ESI-MS measurements can be found in the Supporting Information.

Finally, enhancement in photostability was confirmed via UV−vis spectrometry. The absorption spectrum (Figure SI-24) of avobenzone presents two maxima at 360 and 267 nm corresponding to UVA and UVB regions, respectively, while the absorption spectrum of octinoxate presents two maxima in the UVB region at 299 and 309 nm. In the case of the inclusion complexes $(\beta\text{-CD})_2\cdot$AVO and $(\beta\text{-CD})_3\cdot OCT_2$, the absorption spectrum results from the superimposition of those of the single components (Figure SI-24).

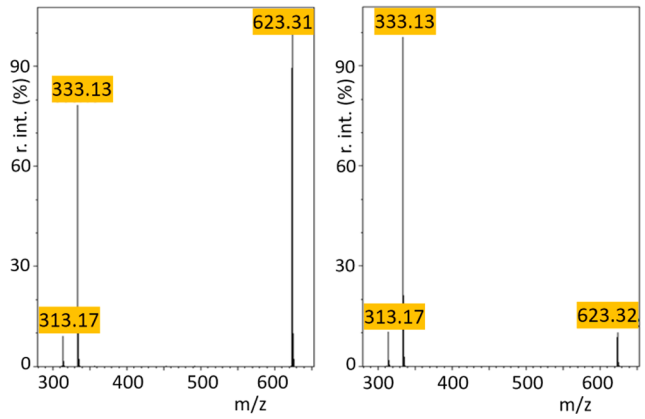

Figure 5. MS/MS spectra with collision energy at 6 eV (left) and 12 eV (right) of the peak at m/z 623 for a mixture of $(\beta\text{-CD})_2\cdot$AVO and $(\beta\text{-CD})_3\cdot OCT_2$ after irradiation.

A physical mixture of avobenzone and octinoxate was irradiated under UV for 24 h, and as previously reported in the literature,[8,9,17] it proved to be unstable, as the corresponding spectrum shows a dramatic change of the absorption in the regions of the two UV filters, with a maximum appearing in the UVC region (Figure SI-25).

Likewise, a physical mixture of $(\beta\text{-CD})_2\cdot$AVO and $(\beta\text{-CD})_3\cdot OCT_2$ was irradiated overnight, and then, the UV−vis spectrum was recorded again. The results, shown in Figure 6, demonstrate that when the two molecules are protected by

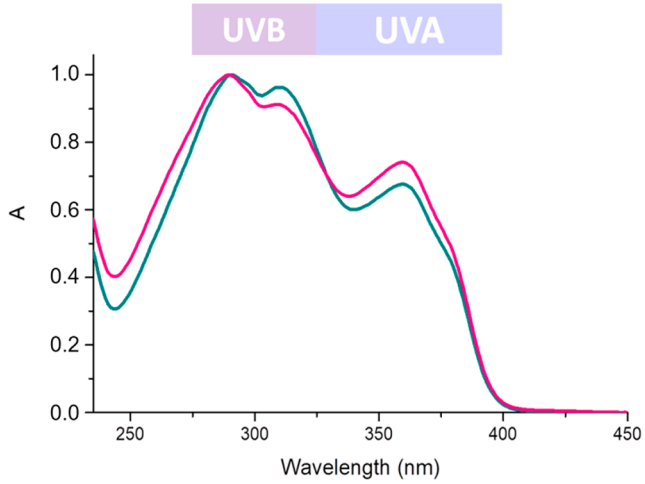

Figure 6. UV−vis spectra of $(\beta\text{-CD})_2\cdot$AVO and $(\beta\text{-CD})_3\cdot OCT_2$ before (green line) and after (pink line) 24 h of irradiation.

β-cyclodextrin, the degradation process is strongly reduced, as can be seen by the unchanged spectra of $(\beta\text{-CD})_2\cdot$AVO and $(\beta\text{-CD})_3\cdot OCT_2$ after irradiation compared to that before irradiation (Figure 6). In fact, there is no evidence of the formation of a peak in the UVC region, and the general outline is unchanged, maintaining AVO and OCT typical bands.

https://dx.doi.org/10.1021/acssuschemeng.0c02735
ACS Sustainable Chem. Eng. 2020, 8, 13215−13225

CONCLUSIONS

In this work, two novel inclusion complexes made up of β-cyclodextrin and two sunscreens, namely, avobenzone and octinoxate, were successfully assembled in the solid-state exploiting the hydrophobic effect to afford the corresponding inclusion complexes. Moreover, during this investigation, a new polymorph (Form II) corresponding to a metastable phase of avobenzone was discovered, fully characterized, and found to be in a monotropic relation with the commercially available Form I.

Although avobenzone and octinoxate, which absorb in the UVA and UVB regions, respectively, are among the most widely used in formulation of sunscreens, they present some drawbacks owing to their tendency to photodegrade under UV exposure leading to a loss of efficacy with time. To overcome this, a common approach is to adjust the photostability by adding other additives or by increasing the amounts of UV filters within the formulations.

Encapsulation of the filters within host molecules that do not interfere with the sunscreen activity may represent a viable option to overcome the photostability issue (Scheme 3).

Scheme 3. Photostability of AVO and OCT Sunscreens Is Dramatically Enhanced upon Inclusion in β-Cyclodextrin

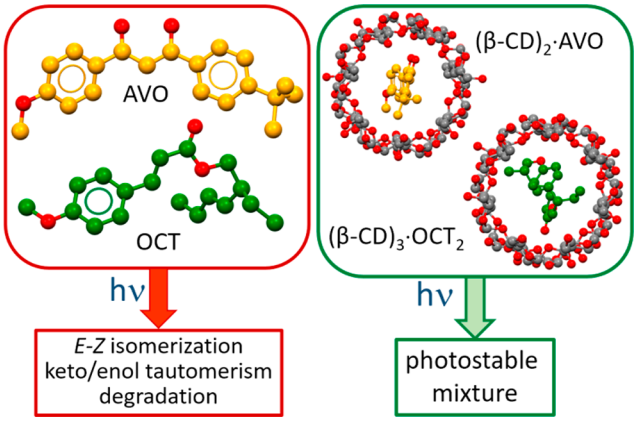

The two β-CD inclusion complexes were obtained through simple, "green", and high yield mechanochemical synthesis (kneading with water), as well as via slurry in water, and fully characterized in the solid state. A combination of solid-state techniques (powder XRD, Raman, thermal analyses) and ^{1}H NMR spectroscopy in solution demonstrated the formation of crystalline inclusion compounds belonging to the C2 isostructural series for β-CD[58,59] and allowed us to assess the respective formulas as $(\beta\text{-CD})_2\cdot$AVO and $(\beta\text{-CD})_3\cdot OCT_2$, with a water content of ca. 8 water molecules each. The photostability of avobenzone and octinoxate within the corresponding inclusion complexes was successfully demonstrated via ESI-MS spectrometry, as no sign of typical photoreaction byproducts are shown after UV irradiation. Finally, UV−vis spectroscopy was used to further confirm the photostability of these compounds and therefore their suitability as sunscreens.

With our study, we have shown that a viable route is feasible for the development of improved sunscreens and is novel in formulation of sunscreens, with special attention to environmentally safe products. The enhanced photostability of the inclusion complexes of avobenzone and octinoxate in β-cyclodextrin would also allow a reduction of the amount of UV filters in sun creams, with potential benefits for the skin and the environment. Further studies are under way to extend this approach to other UVA and UVB filters and to their formulations.

ASSOCIATED CONTENT

Supporting Information

The Supporting Information is available free of charge at https://pubs.acs.org/doi/10.1021/acssuschemeng.0c02735.

XRPD patterns, Pawley refinement plots, Raman and FTIR spectra, X-ray crystallographic data and characterization details for avobenzone Form 2, TGA, and DSC thermograms (PDF)

X-ray crystallographic data for avobenzone Form 2 (CIF)

AUTHOR INFORMATION

Corresponding Authors

Fabrizia Grepioni − *Dipartimento di Chimica "Giacomo Ciamician", Università di Bologna, 40126 Bologna, Italy*; orcid.org/0000-0003-3895-0979; Email: fabrizia.grepioni@unibo.it

Paola Taddei − *Dipartimento di Scienze Biomediche e Neuromotorie, Università di Bologna, 40126 Bologna, Italy*; Email: paola.taddei@unibo.it

Authors

Simone d'Agostino − *Dipartimento di Chimica "Giacomo Ciamician", Università di Bologna, 40126 Bologna, Italy*; orcid.org/0000-0003-3065-5860

Alessandra Azzali − *Dipartimento di Chimica "Giacomo Ciamician", Università di Bologna, 40126 Bologna, Italy*

Lucia Casali − *Dipartimento di Chimica "Giacomo Ciamician", Università di Bologna, 40126 Bologna, Italy*

Complete contact information is available at: https://pubs.acs.org/10.1021/acssuschemeng.0c02735

Author Contributions

The manuscript was written through contributions of all authors. All authors have given approval to the final version of the manuscript.

Notes

The authors declare no competing financial interest.

ACKNOWLEDGMENTS

We thank Dr. Paolo Neviani for his help with MS spectrometry acquisition and analysis and Dr. Stefano Grilli for his help with NMR measurements. Financial support from the University of Bologna is acknowledged.

REFERENCES

(1) Li, C. C.; Lin, L. H.; Lee, H. T.; Tsai, J. R. Avobenzone Encapsulated in Modified Dextrin for Improved UV Protection and Reduced Skin Penetration. *Chem. Pap.* **2016**, *70* (6), 840−847.

(2) González, S.; Fernández-Lorente, M.; Gilaberte-Calzada, Y. The Latest on Skin Photoprotection. *Clin. Dermatol.* **2008**, *26* (6), 614−626.

(3) Sambandan, D. R.; Ratner, D. Sunscreens: An Overview and Update. *J. Am. Acad. Dermatol.* **2011**, *64* (4), 748−758.

(4) Mancuso, J. B.; Maruthi, R.; Wang, S. Q.; Lim, H. W. Sunscreens: An Update. *Am. J. Clin. Dermatol.* **2017**, *18* (5), 643−650.

(5) Dummer, R.; Maier, T. UV Protection and Skin Cancer. In *Cancers of the Skin*; Dummer, R., Nestle, F. O., Burg, G., Eds.; Springer: Berlin, Heidelberg, 2002; pp 7−12.
(6) Krutmann, J.; Passeron, T.; Gilaberte, Y.; Granger, C.; Leone, G.; Narda, M.; Schalka, S.; Trullas, C.; Masson, P.; Lim, H.W. Photoprotection of the Future : Challenges and Opportunities. *J. Eur. Acad. Dermatol. Venereol.* **2020**, *34*, 447−454.
(7) Giacomoni, P. U.; Teta, L.; Najdek, L. Sunscreens: The Impervious Path from Theory to Practice. *Photochem. Photobiol. Sci.* **2010**, *9* (4), 524−529.
(8) Kockler, J.; Oelgemöller, M.; Robertson, S.; Glass, B. D. Photostability of Sunscreens. *J. Photochem. Photobiol., C* **2012**, *13* (1), 91−110.
(9) Serpone, N.; Salinaro, A.; Emeline, A. V.; Horikoshi, S.; Hidaka, H.; Zhao, J. An in Vitro Systematic Spectroscopic Examination of the Photostabilities of a Random Set of Commercial Sunscreen Lotions and Their Chemical UVB/UVA Active Agents. *Photochem. Photobiol. Sci.* **2002**, *1* (12), 970−981.
(10) Serpone, N.; Dondi, D.; Albini, A. Inorganic and Organic UV Filters: Their Role and Efficacy in Sunscreens and Suncare Products. *Inorg. Chim. Acta* **2007**, *360* (3), 794−802.
(11) Damiani, E.; Astolfi, P.; Giesinger, J.; Ehlis, T.; Herzog, B.; Greci, L.; Baschong, W. Assessment of the Photo-Degradation of UV-Filters and Radical-Induced Peroxidation in Cosmetic Sunscreen Formulations. *Free Radical Res.* **2010**, *44* (3), 304−312.
(12) Cozzi, A. C.; Perugini, P.; Gourion-Arsiquaud, S. Comparative Behavior between Sunscreens Based on Free or Encapsulated UV Filters in Term of Skin Penetration, Retention and Photo-Stability. *Eur. J. Pharm. Sci.* **2018**, *121* (June), 309−318.
(13) Hayden, C. G. J.; Cross, S. E.; Anderson, C.; Saunders, N. A.; Roberts, M. S. Sunscreen Penetration of Human Skin and Related Keratinocyte Toxicity after Topical Application. *Skin Pharmacol. Physiol.* **2005**, *18* (4), 170−174.
(14) Pattanaargson, S.; Munhapol, T.; Hirunsupachot, P.; Luangthongaram, P. Photoisomerization of Octyl Methoxycinnamate. *J. Photochem. Photobiol., A* **2004**, *161* (2−3), 269−274.
(15) Pattanaargson, S.; Limphong, P. Stability of Octyl Methoxycinnamate and Identification of Its Photo-Degradation Product. *Int. J. Cosmet. Sci.* **2001**, *23* (3), 153−160.
(16) Cantrell, A.; McGarvey, D. J. Photochemical Studies of 4-Tert-Butyl-4′-Methoxydibenzoylmethane (BM-DBM). *J. Photochem. Photobiol., B* **2001**, *64* (2−3), 117−122.
(17) Dondi, D.; Albini, A.; Serpone, N. Interactions between Different Solar UVB/UVA Filters Contained in Commercial Suncreams and Consequent Loss of UV Protection. *Photochem. Photobiol. Sci.* **2006**, *5* (9), 835−843.
(18) D'Agostino, S.; Boanini, E.; Braga, D.; Grepioni, F. Size Matters: [2 + 2] Photoreactivity in Macro- and Microcrystalline Salts of 4-Aminocinnamic Acid. *Cryst. Growth Des.* **2018**, *18* (4), 2510−2517.
(19) D'Agostino, S.; Taddei, P.; Boanini, E.; Braga, D.; Grepioni, F. Photo- vs Mechano-Induced Polymorphism and Single Crystal to Single Crystal [2 + 2] Photoreactivity in a Bromide Salt of 4-Amino-Cinnamic Acid. *Cryst. Growth Des.* **2017**, *17* (9), 4491−4495.
(20) Afonso, S.; Horita, K.; Sousa E Silva, J. P.; Almeida, I. F.; Amaral, M. H.; Lobão, P. A.; Costa, P. C.; Miranda, M. S.; Esteves Da Silva, J. C. G.; Sousa Lobo, J. M. Photodegradation of Avobenzone: Stabilization Effect of Antioxidants. *J. Photochem. Photobiol., B* **2014**, *140*, 36−40.
(21) Huong, S. P.; Rocher, E.; Fourneron, J. D.; Charles, L.; Monnier, V.; Bun, H.; Andrieu, V. Photoreactivity of the Sunscreen Butylmethoxydibenzoylmethane (DBM) under Various Experimental Conditions. *J. Photochem. Photobiol., A* **2008**, *196* (1), 106−112.
(22) Schwack, W.; Rudolph, T. Photochemistry of Dibenzoyl Methane UVA Filters Part 1. *J. Photochem. Photobiol., B* **1995**, *28* (3), 229−234.
(23) DeAngelo, G. U.S. Patent US8,153,105B1, 2012.
(24) Chodorowski-Kimmes, S. U.S. Patent US2004/0253304A1, 2004.
(25) Chavan, M. V. World Patent WO2012/055678AL, 2012.
(26) Bonda, C. A. World Patent WO2004110394A2, 2004.
(27) Jansen, R.; Osterwalder, U.; Wang, S. Q.; Burnett, M.; Lim, H. W. Photoprotection: Part II. Sunscreen: Development, Efficacy, and Controversies. *J. Am. Acad. Dermatol.* **2013**, *69* (6), 867.e1−867.e14.
(28) Burnett, M. E.; Hu, J. Y.; Wang, S. Q. Sunscreens: Obtaining Adequate Photoprotection. *Dermatol. Ther.* **2012**, *25* (3), 244−251.
(29) Wood, E. *Impacts of Sunscreens on Coral Reefs*; Ocean Grants, 2018.
(30) Schneider, S. L.; Lim, H. W. Review of Environmental Effects of Oxybenzone and Other Sunscreen Active Ingredients. *J. Am. Acad. Dermatol.* **2019**, *80* (1), 266−271.
(31) Danovaro, R.; Bongiorni, L.; Corinaldesi, C.; Giovannelli, D.; Damiani, E.; Astolfi, P.; Greci, L.; Pusceddu, A. Sunscreens Cause Coral Bleaching by Promoting Viral Infections. *Environ. Health Perspect.* **2008**, *116* (4), 441−447.
(32) Janjua, N. R.; Kongshoj, B.; Andersson, A. M.; Wulf, H. C. Sunscreens in Human Plasma and Urine after Repeated Whole-Body Topical Application. *J. Eur. Acad. Dermatol. Venereol.* **2008**, *22* (4), 456−461.
(33) Republic of Palau: Signing Statement SB No 10-135, SDI, HDI. https://www.palaugov.pw/wp-content/uploads/2018/10/RPPL-No.-10-30-re.-The-Responsible-Tourism-Education-Act-of-2018.pdf (accessed Apr 1, 2020).
(34) State of Hawaii: SB No. 2571, SD2, HD2, CD1. https://www.capitol.hawaii.gov/session2018/bills/SB2571_CD1_.htm (accessed Apr 1, 2020).
(35) Ouchene, L.; Litvinov, I. V.; Netchiporouk, E. Hawaii and Other Jurisdictions Ban Oxybenzone or Octinoxate Sunscreens Based on the Confirmed Adverse Environmental Effects of Sunscreen Ingredients on Aquatic Environments. *J. Cutaneous Med. Surg.* **2019**, *23* (6), 648−649.
(36) Adler, B. L.; DeLeo, V. A. Sunscreen Safety: A Review of Recent Studies on Humans and the Environment. *Curr. Dermatol. Rep.* **2020**, *9*, 1.
(37) Palau is first country to ban "reef toxic" sun cream. https://www.bbc.com/news/world-asia-50963080 (accessed Apr 1, 2020).
(38) Kunz, P. Y.; Galicia, H. F.; Fent, K. Comparison of in Vitro and in Vivo Estrogenic Activity of UV Filters in Fish. *Toxicol. Sci.* **2006**, *90* (2), 349−361.
(39) Sánchez-Quiles, D.; Tovar-Sánchez, A. Are Sunscreens a New Environmental Risk Associated with Coastal Tourism? *Environ. Int.* **2015**, *83*, 158−170.
(40) Downs, C. A.; Kramarsky-Winter, E.; Segal, R.; Fauth, J.; Knutson, S.; Bronstein, O.; Ciner, F. R.; Jeger, R.; Lichtenfeld, Y.; Woodley, C. M.; Pennington, P.; Cadenas, K.; Kushmaro, A.; Loya, Y. Toxicopathological Effects of the Sunscreen UV Filter, Oxybenzone (Benzophenone-3), on Coral Planulae and Cultured Primary Cells and Its Environmental Contamination in Hawaii and the U.S. Virgin Islands. *Arch. Environ. Contam. Toxicol.* **2016**, *70* (2), 265−288.
(41) Locke, B.; Jachowicz, J. Fading of Artificial Hair Colour and Its Prevention by Photofilters. *Int. J. Cosmet. Sci.* **2006**, *28* (3), 231−232.
(42) Coelho, L.; Almeida, I. F.; Sousa Lobo, J. M.; Sousa e Silva, J. P. Photostabilization Strategies of Photosensitive Drugs. *Int. J. Pharm.* **2018**, *541* (1−2), 19−25.
(43) Trellu, C.; Mousset, E.; Pechaud, Y.; Huguenot, D.; van Hullebusch, E. D.; Esposito, G.; Oturan, M. A. Removal of Hydrophobic Organic Pollutants from Soil Washing/Flushing Solutions: A Critical Review. *J. Hazard. Mater.* **2016**, *306*, 149−174.
(44) Li, L.; Liu, H.; Li, W.; Liu, K.; Tang, T.; Liu, J.; Jiang, W. One-Step Synthesis of an Environment-Friendly Cyclodextrin-Based Nanosponge and Its Applications for the Removal of Dyestuff from Aqueous Solutions. *Res. Chem. Intermed.* **2020**, *46* (3), 1715−1734.
(45) Biloti, D. N.; Dos Reis, M. M.; Ferreira, M. M. C.; Pessine, F. B. T. Photochemical Behavior under UVA Radiation of β-Cyclodextrin Included Parsol® 1789 with a Chemometric Approach. *J. Mol. Struct.* **1999**, *480*−*481*, 557−561.
(46) Scalia, S.; Villani, S.; Casolari, A. Inclusion Complexation of the Sunscreen Agent 2-Ethylhexyl-<I > p</I>-Dimethylaminobenzoate

with Hydroxypropyl-β-Cyclodextrin: Effect on Photostability. *J. Pharm. Pharmacol.* **1999**, *51* (12), 1367−1374.
(47) Scalia, S.; Casolari, A.; Iaconinoto, A.; Simeoni, S. Comparative Studies of the Influence of Cyclodextrins on the Stability of the Sunscreen Agent, 2-Ethylhexyl-p-Methoxycinnamate. *J. Pharm. Biomed. Anal.* **2002**, *30* (4), 1181−1189.
(48) Mori, T.; Tsuchiya, R.; Doi, M.; Nagatani, N.; Tanaka, T. Solubilization of Ultraviolet Absorbers by Cyclodextrin and Their Potential Application in Cosmetics. *J. Inclusion Phenom. Macrocyclic Chem.* **2019**, *93* (1−2), 91−96.
(49) Srinivasan, K.; Radhakrishnan, S.; Stalin, T. Inclusion Complexes of β-Cyclodextrin-Dinitrocompounds as UV Absorber for Ballpoint Pen Ink. *Spectrochim. Acta, Part A* **2014**, *129*, 551−564.
(50) Scalia, S.; Tursilli, R.; Bianchi, A.; Nostro, P. L.; Bocci, E.; Ridi, F.; Baglioni, P. Incorporation of the Sunscreen Agent, Octyl Methoxycinnamate in a Cellulosic Fabric Grafted with β-Cyclodextrin. *Int. J. Pharm.* **2006**, *308* (1−2), 155−159.
(51) Simeoni, S.; Scalia, S.; Tursilli, R.; Benson, H. Influence of Cyclodextrin Complexation on the in Vitro Human Skin Penetration and Retention of the Sunscreen Agent, Oxybenzone. *J. Inclusion Phenom. Mol. Recognit. Chem.* **2006**, *54* (3−4), 275−282.
(52) Sealy, C. Nanoparticles Keep Sunscreen on the Skin. *Mater. Today* **2016**, *19* (2), 66−67.
(53) Braga, D.; Grepioni, F.; Maini, L.; d'Agostino, S. From Solid-State Structure and Dynamics to Crystal Engineering. *Eur. J. Inorg. Chem.* **2018**, *2018* (32), 3597−3605.
(54) Dolomanov, O. V.; Bourhis, L. J.; Gildea, R. J.; Howard, J. A. K.; Puschmann, H. OLEX2: A Complete Structure Solution, Refinement and Analysis Program. *J. Appl. Crystallogr.* **2009**, *42* (2), 339−341.
(55) Macrae, C. F.; Edgington, P. R.; McCabe, P.; Pidcock, E.; Shields, G. P.; Taylor, R.; Towler, M.; van de Streek, J. Mercury: Visualization and Analysis of Crystal Structures. *J. Appl. Crystallogr.* **2006**, *39* (3), 453−457.
(56) Groom, C. R.; Bruno, I. J.; Lightfoot, M. P.; Ward, S. C. The Cambridge Structural Database. *Acta Crystallogr., Sect. B: Struct. Sci., Cryst. Eng. Mater.* **2016**, *72* (2), 171−179.
(57) Coelho, A. A. *TOPAS-Academic V4.1*; Coelho Software: Brisbane, Australia, 2007.
(58) Smith, V. J.; Rougier, N. M.; de Rossi, R. H.; Caira, M. R.; Buján, E. I.; Fernández, M. A.; Bourne, S. A. Investigation of the Inclusion of the Herbicide Metobromuron in Native Cyclodextrins by Powder X-Ray Diffraction and Isothermal Titration Calorimetry. *Carbohydr. Res.* **2009**, *344* (17), 2388−2393.
(59) Caira, M. R. On the Isostructurality of Cyclodextrin Inclusion Complexes and Its Practical Utility. *Rev. Roum. Chim.* **2001**, *46*, 371−386.
(60) Yuan, L.; Li, S.; Huo, D.; Zhou, W.; Wang, X.; Bai, D.; Hu, J. Studies on the Preparation and Photostability of Avobenzone and (2-Hydroxy)Propyl-β-Cyclodextrin Inclusion Complex. *J. Photochem. Photobiol., A* **2019**, *369*, 174−180.
(61) Caira, M. R.; Nassimbeni, L. R. *Comprehensive Supramolecular Chemistry*; Atwood, J. L., Davies, J. E. D., MacNicol, D. D., Vögtle, F., Eds.; Elsevier Science: Oxford, 1996; pp 825−850.
(62) Braga, S. S.; Gonçalves, I. S.; Herdtweck, E.; Teixeira-Dias, J. J. C. Solid State Inclusion Compound of S-Ibuprofen in β-Cyclodextrin: Structure and Characterisation. *New J. Chem.* **2003**, *27* (3), 597−601.
(63) Moraes, C. M.; Abrami, P.; De Araujo, D. R.; Braga, A. F. A.; Issa, M. G.; Ferraz, H. G.; De Paula, E.; Fraceto, L. F. Characterization of Lidocaine:Hydroxypropyl-β-Cyclodextrin Inclusion Complex. *J. Inclusion Phenom. Mol. Recognit. Chem.* **2007**, *57* (1−4), 313−316.
(64) Cruickshank, D.; Rougier, N. M.; Vico, R. V.; Rossi, R. H. d.; Buján, E. I.; Bourne, S. A.; Caira, M. R. Solid-State Structures and Thermal Properties of Inclusion Complexes of the Organophosphate Insecticide Fenitrothion with Permethylated Cyclodextrins. *Carbohydr. Res.* **2010**, *345* (1), 141−147.
(65) Caira, M. R.; Hunter, R.; Bourne, S. A.; Smith, V. J. Preparation, Thermal Behaviour and Solid-State Structures of Inclusion Complexes of Permethylated-β-Cyclodextrin with the Garlic-Derived Antithrombotics (E)- and (Z)-Ajoene. *Supramol. Chem.* **2004**, *16* (6), 395−403.
(66) Rácz, C. P.; Borodi, G.; Pop, M. M.; Kacso, I.; Sánta, S.; Tomoaia-Cotisel, M. Structure of the Inclusion Complex of B-Cyclodextrin with Lipoic Acid from Laboratory Powder Diffraction Data. *Acta Crystallogr., Sect. B: Struct. Sci.* **2012**, *68* (2), 164−170.
(67) Ramos, A. I.; Braga, T. M.; Silva, P.; Fernandes, J. A.; Ribeiro-Claro, P.; De Fátima Silva Lopes, M.; Paz, F. A. A.; Braga, S. S. Chloramphenicol·cyclodextrin Inclusion Compounds: Co-Dissolution and Mechanochemical Preparations and Antibacterial Action. *CrystEngComm* **2013**, *15* (15), 2822−2834.
(68) Bethanis, K.; Tzamalis, P.; Tsorteki, F.; Kokkinou, A.; Christoforides, E.; Mentzafos, D. Structural Study of the Inclusion Compounds of Thymol, Carvacrol and Eugenol in β-Cyclodextrin by X-Ray Crystallography. *J. Inclusion Phenom. Macrocyclic Chem.* **2013**, *77* (1−4), 163−173.
(69) Beyere, L.; Yarasi, S.; Loppnow, G. R. Solvent Effects on Sunscreen Active Ingredients Using Raman Spectroscopy. *J. Raman Spectrosc.* **2003**, *34* (10), 743−750.
(70) Russell, N. R.; McNamara, M. FT-IR and Raman Spectral Evidence for Metal Complex Formation with β-Cyclodextrin as a First Sphere Ligand. *J. Inclusion Phenom. Mol. Recognit. Chem.* **1989**, *7* (4), 455−460.
(71) Costa, M. M.; Alves, L. P.; Osório, R. A. L.; Pacheco, M. T. T.; Silveira, L. Detecting Active Ingredients of Insect Repellents and Sunscreens Topically in Skin by Raman Spectroscopy. *J. Biomed. Opt.* **2018**, *23* (10), 1.
(72) Tayyari, S. F.; Rahemi, H.; Nekoei, A. R.; Zahedi-Tabrizi, M.; Wang, Y. A. Vibrational Assignment and Structure of Dibenzoylmethane. A Density Functional Theoretical Study. *Spectrochim. Acta, Part A* **2007**, *66* (2), 394−404.
(73) Hammond, G. S.; Borduin, W. G.; Guter, G. A. Chelates of β-Diketones. I. Enolization, Ionization and Spectra. *J. Am. Chem. Soc.* **1959**, *81* (17), 4682−4686.
(74) Rachmawati, H.; Edityaningrum, C. A.; Mauludin, R. Molecular Inclusion Complex of Curcumin-β-Cyclodextrin Nanoparticle to Enhance Curcumin Skin Permeability from Hydrophilic Matrix Gel. *AAPS PharmSciTech* **2013**, *14* (4), 1303−1312.
(75) Mohan, P. R. K.; Sreelakshmi, G.; Muraleedharan, C. V.; Joseph, R. Water Soluble Complexes of Curcumin with Cyclodextrins: Characterization by FT-Raman Spectroscopy. *Vib. Spectrosc.* **2012**, *62*, 77−84.
(76) Karpkird, T.; Khunsakorn, R.; Noptheeranuphap, C.; Midpanon, S. Inclusion Complexes and Photostability of UV Filters and Curcumin with Beta-Cyclodextrin Polymers: Effect on Cross-Linkers. *J. Inclusion Phenom. Macrocyclic Chem.* **2018**, *91* (1−2), 37−45.
(77) Karpkird, T.; Khunsakorn, R.; Noptheeranuphap, C.; Jettanasen, J. Photostability of Water-Soluble Inclusion Complexes of UV-Filters and Curcumin with Gamma-Cyclodextrin Polymer. *J. Inclusion Phenom. Macrocyclic Chem.* **2016**, *84* (1−2), 121−128.
(78) Al-Rawashdeh, N. A. F. F.; Al-Sadeh, K. S.; Al-Bitar, M. B. Inclusion Complexes of Sunscreen Agents with β-Cyclodextrin: Spectroscopic and Molecular Modeling Studies. *J. Spectrosc.* **2013**, *2013* (1), 1.
(79) Ricci-Junior, E.; Monteiro; Ozzetti; Vergnanini; Volpato; Gitirana, L.; Freitas; Santos, E. P. Evaluation of Octyl P-Methoxycinnamate Included in Liposomes and Cyclodextrins in Anti-Solar Preparations: Preparations, Characterizations and in Vitro Penetration Studies. *Int. J. Nanomed.* **2012**, *7*, 3045−3058.
(80) Baglole, K. N.; Boland, P. G.; Wagner, B. D. Fluorescence Enhancement of Curcumin upon Inclusion into Parent and Modified Cyclodextrins. *J. Photochem. Photobiol., A* **2005**, *173*, 230−237.
(81) López-Tobar, E.; Blanch, G. P.; Ruiz Del Castillo, M. L.; Sanchez-Cortes, S. Encapsulation and Isomerization of Curcumin with Cyclodextrins Characterized by Electronic and Vibrational Spectroscopy. *Vib. Spectrosc.* **2012**, *62*, 292−298.

https://dx.doi.org/10.1021/acssuschemeng.0c02735
ACS Sustainable Chem. Eng. 2020, 8, 13215−13225

(82) Szejtli, J. Introduction and General Overview of Cyclodextrin Chemistry. *Chem. Rev.* **1998**, *98* (5), 1743−1753.
(83) Ferreira, I. R.; Ando, R. A. Shifting the Azo-Hydrazone Tautomeric Equilibrium of Methyl Yellow in Acidic Medium by the Formation of Inclusion Complexes with Cyclodextrins. *Chem. Phys. Lett.* **2012**, *522*, 51−53.

https://dx.doi.org/10.1021/acssuschemeng.0c02735
ACS Sustainable Chem. Eng. 2020, 8, 13215−13225